Vibrational fine structure of C_5 via anion slow photoelectron velocity-map imaging

Marissa L. Weichman,[1] Jongjin B. Kim,[1] and Daniel M. Neumark[1,2,a)]
[1]*Department of Chemistry, University of California, Berkeley, California 94720, USA*
[2]*Chemical Sciences Division, Lawrence Berkeley National Laboratory, Berkeley, California 94720, USA*

(Received 3 August 2013; accepted 25 September 2013; published online 10 October 2013)

High-resolution anion photoelectron spectra of cryogenically cooled C_5^- clusters are reported using slow photoelectron velocity-map imaging spectroscopy. We resolve vibronic transitions to the ν_2 stretching mode and multiply excited ν_5, ν_6, and ν_7 bending modes of neutral C_5 with significantly higher accuracy than previous experiments. Weak transitions to Franck-Condon (FC) forbidden singly excited bending modes are made possible by Herzberg-Teller coupling between electronic states of the neutral cluster. In addition, we resolve vibrational fine structure corresponding to different angular momentum states of multiply excited bending modes. The observation of this multiplet structure, some of which is FC forbidden, is attributed to Renner-Teller coupling between vibrational levels in the C_5^- ground electronic state. © *2013 AIP Publishing LLC*. [http://dx.doi.org/10.1063/1.4824657]

I. INTRODUCTION

Carbon clusters (C_n) have been of great interest in interstellar, plasma, and combustion chemistry for over three decades.[1–5] They represent one of the most important families of clusters owing to their relevance and structural complexity. Many state-of-the-art experimental and theoretical methods were developed with carbon clusters as their primary target and were subsequently extended to other systems. Following this paradigm, we recently reported a study of the neutral C_5 cluster via high-resolution slow photoelectron velocity-map imaging spectroscopy of cryo-cooled C_5^- anions in order to demonstrate the power of this combination of techniques.[6,7] Here, we present a more complete spectroscopic study of C_5 and C_5^- using the same method.

Small carbon clusters with an odd number of atoms tend to have linear geometries, while even-numbered clusters also have low-energy ring structures.[8–10] Larger clusters can preferentially form rings and fullerenes.[11,12] The neutral C_5 cluster is a linear cumulene with a $^1\Sigma_g^+$ ground electronic state.[9,13,14] C_5 was first detected experimentally by its ν_3 anti-symmetric stretching mode in cold neon and argon matrices.[15] Soon afterwards, the same ν_3 mode was identified in the gas phase from the absorption spectrum of the circumstellar shell of a carbon star[16] and in the laboratory using infrared diode laser absorption spectroscopy.[17,18] Electronic and vibrational levels of C_5 have since been investigated with further rare gas matrix studies,[19–21] cavity ringdown spectroscopy,[22] resonant two-photon ionization spectroscopy,[23] and electronic structure calculations.[10,24–29] The C_5^- anion is also linear, with a $^2\Pi_u$ ground state.[30,31] While not as well-characterized as its neutral counterpart, its electronic and vibrational structure has been investigated with multiphoton electron detachment,[32–34] matrix IR absorption,[35–37] and various theoretical methods.[38–40]

Anion photoelectron spectroscopy (PES) is an attractive technique for clusters in general[41,42] as a means of probing the electron affinity and vibronic structure of size-selected neutral species. The vibrational structure in a PE spectrum is sensitive to the change in geometry of a cluster upon photodetachment, and is often complementary to IR spectroscopy because it is dominated by progressions in totally symmetric vibrational modes. Previous PES studies of C_5^- have been reported by Yang *et al.*[43] at a resolution of ~1000 cm^{-1}, by Arnold *et al.*[44] with a resolution of ~100 cm^{-1}, and by Kitsopoulos *et al.*[45] with zero electron kinetic energy (ZEKE) spectroscopy, at a resolution of 10−30 cm^{-1}. The ZEKE study resolved transitions to the ν_2 (779 cm^{-1}), $2\nu_5$ (432 cm^{-1}), $2\nu_6$ (1070 cm^{-1}), and $2\nu_7$ (212 cm^{-1}) vibrational states of neutral C_5, as well as a spin-orbit (SO) splitting of 22 cm^{-1} between the $^2\Pi_{1/2u}$ and $^2\Pi_{3/2u}$ levels of the C_5^- ground electronic state.

In the present work, we report high-resolution slow photoelectron velocity-map imaging (SEVI) vibronic spectra of C_5^-, cooled in our cryogenic ion trap. We previously focused on the spin-orbit levels of the $\tilde{X}^1\Sigma_g^+ \leftarrow \tilde{X}^2\Pi_u$ (neutral ← anion) vibrational origin to demonstrate the cooling ability of the ion trap, finding a SO splitting of 25 cm^{-1} and an internal ion temperature as low as 10 K.[6] Here, the entire $\tilde{X}^1\Sigma_g^+ \leftarrow \tilde{X}^2\Pi_u$ photodetachment band is considered. The combination of cryogenic cooling with the inherent high instrumental resolution of SEVI (<4 cm^{-1}) reveals considerably more vibrational structure of neutral C_5 than was seen in previous studies. We find ν_2 (780 cm^{-1}), $2\nu_5$ (408 cm^{-1}), $2\nu_6$ (1069 cm^{-1}), and $2\nu_7$ (208 cm^{-1}), and assign newly observed combination bands. We resolve vibrational fine structure with splittings as small as 6 cm^{-1} corresponding to doubly excited levels of the ν_5, ν_6, and ν_7 bending modes with different values of vibrational angular momentum. Additionally, a number of Franck-Condon (FC) forbidden peaks are seen that provide

a)Author to whom correspondence should be addressed. Electronic mail: dneumark@berkeley.edu

evidence of subtle vibronic coupling effects in both the neutral and anion clusters. Coupled cluster electronic structure theory calculations and Franck-Condon simulations aid in interpreting the experimental spectra.

II. EXPERIMENTAL METHODS

The SEVI method has been described in detail previously,[46,47] as has the current experimental setup in our laboratory.[6] Briefly, SEVI is a high-resolution variant of photoelectron spectroscopy, wherein anions are photodetached with a tunable laser. Photoelectrons are extracted and imaged in a velocity-map imaging (VMI) apparatus. At low extraction voltages, slow electrons are preferentially detected and magnified on the imaging detector, resulting in considerably higher kinetic energy resolution than conventional VMI.

C_5^- clusters were generated with a laser vaporization cluster source. A frequency-doubled Nd:YAG laser was focused onto a 1 in. disc of graphite, producing a carbon plasma that was entrained within a pulse of He buffer gas from an Even-Lavie solenoid valve.[48] The resulting pulsed jet of carbon clusters passed through a skimmer. Anions were directed through a radio frequency (RF) ion guide and a quadrupole mass spectrometer to provide rough mass selection for the cluster size of interest en route to the linear octupole ion trap.[6] Here, the ions were trapped radially by alternating RF voltages applied to the trap rods[49] and axially by entrance and exit electrodes held at low DC voltages. The ion trap was in thermal contact with a closed-cycle refrigerator cooled to 5 K. Prior to admitting the ions, the trap was filled with a pulsed burst of He/H_2 buffer gas in a 80:20 mixture, precooled to 40 K. The ions were stored in the trap for ~38 ms before extraction into a Wiley-McLaren time-of-flight mass spectrometer (TOFMS);[50] this trapping time enabled collisional thermalization of the ions to their ground vibrational state.

The TOFMS spatially and temporally focused the ion packet into the laser interaction region of the SEVI spectrometer. A mass gate ensured that only the desired $^{12}C_5^-$ clusters entered the interaction region. The ion packet was then photodetached with the frequency-doubled output of an Nd:YAG-pumped tunable dye laser. The resulting photoelectrons were focused with a velocity-map imaging electrostatic lens[51] onto a detector consisting of two chevron-stacked micro-channel plates (MCPs) coupled to a phosphor screen.[52] Images of the screen were collected by a 1024 × 768 pixel CCD camera and sent to a computer running NuACQ software provided by the Suits group[53] that was modified to suit our experiment. During data acquisition, we used an event counting algorithm[54] to identify spots corresponding to single electron events and compute their centroids in real time. Event counting enhances spatial resolution and reduces effects from background noise and inhomogeneity in the response of the CCD and MCPs. The centroid of each spot was accumulated to create an image which was subsequently centered, smoothed, and quadrant-symmetrized.

The 3D distribution of electron velocity vectors was reconstructed from the 2D accumulated image using an inverse-Abel method.[55] The reconstructed image was then integrated angularly to obtain a spectrum. The distance of an electron spot from the center of the image is linearly proportional to the electron speed. The apparatus was calibrated with SEVI images of well-known photodetachment transitions[56] of atomic F^- at a variety of photon energies, in order to relate the distance from the image center in pixels to electron kinetic energy (eKE) for a given VMI extraction voltage. The features occurring at lowest eKE in our spectra correspond to transitions to neutral states with the highest internal energy. As the eKE depends on photodetachment laser energy ($h\nu$), we report SEVI spectra as a function of electron binding energy (eBE), given by $eBE = h\nu - eKE$.

The VMI spectrometer has an approximately constant resolving power $\Delta eKE/eKE$. Hence, its resolution is best for transitions closest to threshold (low eKE). As described in more detail in Ref. 57, in order to construct a high resolution SEVI spectrum covering the entire band, we first obtained a low-resolution overview spectrum at a single photon energy. We then obtained high-resolution photodetachment spectra over relatively narrow eKE windows by measuring spectra at a series of photodetachment energies lying just above features of interest. These windows were combined to create a composite high-resolution spectrum of the entire band.

III. CALCULATIONS

Electronic structure theory calculations for C_5 and C_5^- were carried out at the RCCSD(T)/aug-cc-pVTZ level of theory[58–60] in order to determine the geometries, normal modes, and harmonic frequencies of both species. All calculations were carried out using the Molpro 2010.1 software package.[61] Clusters were restricted to linear geometries, as recommended by prior theoretical and experimental work.[9,14,44,45] Calculated electronic term energies were zero-point vibrational energy corrected.

The photoelectron spectrum for the $\tilde{X}^1\Sigma_g^+ \leftarrow \tilde{X}^2\Pi_u$ photodetachment of C_5^- was simulated using the ezSpectrum v3.0 software package.[62] All modes were treated in the harmonic approximation and FC overlap factors were calculated using full Duschinsky mixing of all normal modes.[63] The vibrational origin was fixed to the experimentally determined value of 23 018 cm^{-1} (2.8538 eV).[6] Those frequencies of neutral C_5 that were observed in the SEVI spectra (ν_2, $2\nu_5$, $2\nu_6$, and $2\nu_7$) were scaled to their experimental values; the others were left at their calculated RCCSD(T)/aug-cc-pVTZ values.

As C_5^- has a $^2\Pi_u$ electronic ground state, Renner-Teller (RT) and spin-orbit effects must be taken into account when considering the anion bending vibrational modes. In this work, the bending frequencies of C_5^- were taken from Perić *et al.*,[40] in which the authors included these effects in modeling the C_5^- anion bending potentials to obtain better values for the ν_5, ν_6, and ν_7 frequencies. The anion stretch frequencies were left at their calculated RCCSD(T)/aug-cc-pVTZ values.

IV. RESULTS

The SEVI spectra of the $\tilde{X}^1\Sigma_g^+ \leftarrow \tilde{X}^2\Pi_u$ photodetachment of C_5^-, taken at an ion trap temperature of 5 K, are presented in Fig. 1. A low-resolution overview spectrum at

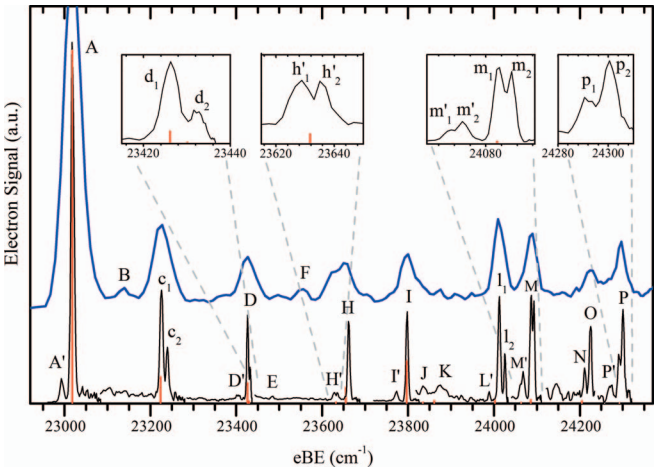

FIG. 1. SEVI spectra of the $\tilde{X}^1\Sigma_g^+ \leftarrow \tilde{X}^2\Pi_u$ photodetachment of C_5^-, taken with the ion trap held at 5 K. A low-resolution overview spectrum is shown in blue. The black trace is a high-resolution composite spectrum taken at many laser frequencies. A FC simulation stick spectrum is shown in red.

photon energy $h\nu = 24\,728$ cm^{-1} is shown in blue. The black traces constitute the high-resolution composite spectrum constructed as described in Sec. II. The high-resolution traces are scaled to fit the intensity profile of the overview and are vertically offset for comparison. A FC simulation stick spectrum is shown in red, scaled to match the intensity of peak A.

The spectra are dominated by a single peak at low eBE (peak A), above which we resolve narrow vibrational features covering ~1500 cm^{-1}. A much weaker peak (peak A′) lies 25 cm^{-1} below peak A. No spectroscopic features are visible below peaks A′/A, indicating that they represent the $\tilde{X}^1\Sigma_g^+ \leftarrow \tilde{X}^2\Pi_u$ vibrational origin, with peak A′ originating from the $^2\Pi_{3/2u}$ upper spin-orbit level of the anion, in agreement with previous findings.[6,45] Typical experimental peak linewidths are 5−9 cm^{-1} FWHM, far narrower than previous photodetachment experiments. Additionally, at high resolution, some features (peaks C, D, L, M, and P) resolve into previously unseen multiplets with splittings as small as 6 cm^{-1}.

Most observed peaks in the accumulated images have isotropic photoelectron angular distributions (PADs). This is consistent with the PAD expected of a $^1\Sigma_g^+ \leftarrow {}^2\Pi_u$ photodetachment process.[64,65] Only peaks B and F appear to have anisotropic PADs, aligned parallel to the laser polarization axis. Peaks B and F are only weakly visible in the overview spectrum, and are not seen in the higher resolution composite spectrum.

Positions and assignments for the peaks labeled in Fig. 1 are summarized in Table I. Calculated and experimental parameters for C_5^- and C_5 obtained in this work are summarized in Table II and generally found to be in good agreement with literature values.[3,27,38–40]

V. DISCUSSION

The C_5^- SEVI spectra presented in Fig. 1 are a significant improvement over the ZEKE spectrum obtained by Kitsopoulos *et al.* in 1991.[45] The experimental resolution is substantially better (2−4 cm^{-1} in the current work as compared to 10−30 cm^{-1} in the ZEKE experiment), enabling better separation of well-defined doublets (A′/A, D′/D, etc.) from the two spin-orbit components of the anion. In addition, even finer multiplet structure of many vibrational modes is seen that was not resolved in the ZEKE spectrum. As these multiplets occur in bending modes with more than one quantum of vibrational excitation, it is likely that they arise from closely spaced vibrational angular momentum states with the same principal quantum number.

The improved resolution of the C_5^- spectra presented here results from several improvements to the SEVI apparatus. The addition of event counting to our data acquisition process increases our sensitivity and enhances VMI spatial resolution. Cryogenic cooling of anions in our trap prior to photodetachment eliminates vibrational hot bands and dramatically narrows rotational envelopes. As described previously,[6] the internal anion temperature can be quantified by comparing the relative intensity of peaks corresponding to photodetachment from the $^2\Pi_{1/2u}$ and $^2\Pi_{3/2u}$ spin-orbit levels of the C_5^- electronic ground state. Assuming that the anions are thermalized in the ion trap, the relative populations of these two states

TABLE I. Peak positions, offsets, and assignments for the SEVI spectra of C_5^- given in Fig. 1.

Peak		eBE (cm^{-1})	Offset (cm^{-1})	Assignment	Electronic band
A′		22 993	−25	0_0^0	$^1\Sigma_g^+ \leftarrow {}^2\Pi_{3/2u}$
A		23 018	0	0_0^0	$^1\Sigma_g^+ \leftarrow {}^2\Pi_{1/2u}$
B		23 137	119	7_0^1	$^1\Sigma_g^+ \leftarrow {}^2\Pi_{1/2u}$
C	c_1	23 226	208	7_0^2 ($l_7 = 0$)	$^1\Sigma_g^+ \leftarrow {}^2\Pi_{1/2u}$
	c_2	23 240	222	7_0^2 ($l_7 = \pm 2$)	$^1\Sigma_g^+ \leftarrow {}^2\Pi_{1/2u}$
D′		23 403	385	5_0^2	$^1\Sigma_g^+ \leftarrow {}^2\Pi_{3/2u}$
D	d_1	23 426	408	5_0^2 ($l_5 = 0$)	$^1\Sigma_g^+ \leftarrow {}^2\Pi_{1/2u}$
	d_2	23 432	414	5_0^2 ($l_5 = \pm 2$)	$^1\Sigma_g^+ \leftarrow {}^2\Pi_{1/2u}$
E		23 483	465	7_0^4	$^1\Sigma_g^+ \leftarrow {}^2\Pi_{1/2u}$
F		23 553	535	6_0^1	$^1\Sigma_g^+ \leftarrow {}^2\Pi_{1/2u}$
H′	h_1'	23 628	610	$5_0^2 7_0^2$	$^1\Sigma_g^+ \leftarrow {}^2\Pi_{1/2u}$
	h_2'	23 636	618	$6_0^1 7_0^1$	$^1\Sigma_g^+ \leftarrow {}^2\Pi_{3/2u}$
H		23 662	644	$6_0^1 7_0^1$	$^1\Sigma_g^+ \leftarrow {}^2\Pi_{1/2u}$
I′		23 773	755	2_0^1	$^1\Sigma_g^+ \leftarrow {}^2\Pi_{3/2u}$
I		23 798	780	2_0^1	$^1\Sigma_g^+ \leftarrow {}^2\Pi_{1/2u}$
J		23 835	817	5_0^4	$^1\Sigma_g^+ \leftarrow {}^2\Pi_{1/2u}$
K		23 876	858	$6_0^1 7_0^3$	$^1\Sigma_g^+ \leftarrow {}^2\Pi_{1/2u}$
L′		23 989	971	$2_0^1 7_0^2$	$^1\Sigma_g^+ \leftarrow {}^2\Pi_{3/2u}$
L	l_1	24 012	994	$2_0^1 7_0^2$ ($l_7 = 0$)	$^1\Sigma_g^+ \leftarrow {}^2\Pi_{1/2u}$
	l_2	24 026	1008	$2_0^1 7_0^2$ ($l_7 = \pm 2$)	$^1\Sigma_g^+ \leftarrow {}^2\Pi_{1/2u}$
M′	m_1'	24 061	1043	6_0^2 ($l_6 = 0$)	$^1\Sigma_g^+ \leftarrow {}^2\Pi_{3/2u}$
	m_2'	24 068	1050	6_0^2 ($l_6 = \pm 2$)	$^1\Sigma_g^+ \leftarrow {}^2\Pi_{3/2u}$
M	m_1	24 087	1069	6_0^2 ($l_6 = 0$)	$^1\Sigma_g^+ \leftarrow {}^2\Pi_{1/2u}$
	m_2	24 093	1075	6_0^2 ($l_6 = \pm 2$)	$^1\Sigma_g^+ \leftarrow {}^2\Pi_{1/2u}$
N		24 212	1194	$2_0^1 5_0^2$	$^1\Sigma_g^+ \leftarrow {}^2\Pi_{1/2u}$
O		24 225	1207	$2_0^1 7_0^4$	$^1\Sigma_g^+ \leftarrow {}^2\Pi_{1/2u}$
P′		24 272	1254	$6_0^2 7_0^2$	$^1\Sigma_g^+ \leftarrow {}^2\Pi_{3/2u}$
P	p_1	24 291	1273	$6_0^2 7_0^2$ ($l_6, l_7 = ?$)	$^1\Sigma_g^+ \leftarrow {}^2\Pi_{1/2u}$
	p_2	24 301	1283	$6_0^2 7_0^2$ ($l_6, l_7 = ?$)	$^1\Sigma_g^+ \leftarrow {}^2\Pi_{1/2u}$

TABLE II. Calculated and experimental parameters for C_5^- and C_5 found in this work. Frequencies are in wavenumbers (cm^{-1}) and bond lengths are in Ångströms (Å). The given uncertainties are one standard deviation of a Gaussian fit to the experimentally observed peak. All calculated parameters were obtained at the RCCSD(T)/aug-cc-pVTZ level of theory, with the exception of the values taken from Ref. 40.

Parameter	C_5^- calculated	C_5 calculated	C_5 experimental	
$R_{C-C,\ inner}$	1.307	1.289		
$R_{C-C,\ outer}$	1.293	1.297		
ν_1 (σ_g^+)	1976	1977		
ν_2 (σ_g^+)	748	772	$\nu_2 = 780(3)$	
ν_3 (σ_u^+)	1986	2213		
ν_4 (σ_u^+)	1417	1442		
ν_5 (π_g)	(255, 351) 334[a]	196	$2\nu_5 = 408(2)$	$4g_{55} = 6$
ν_6 (π_u)	(333, 545) 521[a]	517	$\nu_6 = 535(13)$; $2\nu_6 = 1069(3)$	$4g_{66} = 7$
ν_7 (π_u)	(123, 135) 158[a]	109	$\nu_7 = 119(9)$; $2\nu_7 = 208(4)$	$4g_{77} = 14$
EA		22428	$^1\Sigma_g^+ \leftarrow {}^2\Pi_{1/2u}$: 23018(3)	
			$^1\Sigma_g^+ \leftarrow {}^2\Pi_{3/2u}$: 22993(3)	

[a]Frequencies for anion bending modes taken from Perić *et al.*[40]

should be governed by Maxwell-Boltzmann statistics. The ZEKE study measured a spin-orbit temperature of 30 K under optimal conditions. Previously, we were able to optimize the cooling conditions in our ion trap to achieve an ion temperature of 10 K at the time of photodetachment.[6] The spectra presented here have a slightly higher SO temperature of 13 K as the system was tuned to optimize both ion temperature and signal.

The spectra are dominated by the vibrational origin (peak A), which indicates that the geometry change between anion and neutral is minimal. The calculated geometries outlined in Table II correspondingly predict changes in C–C bond lengths of at most ∼1% upon photodetachment. The peak assignments in Table I were informed by the results of *ab initio* calculations and assignments from previous studies.[44,45] Experimental and simulated peak positions are generally in good agreement, but the simulation systematically underestimates the intensities for transitions to vibrationally excited states, especially those involving multiply excited bending modes. Peaks designated "prime" correspond to transitions originating from the $^2\Pi_{3/2u}$ SO level of C_5^-, with the exception of peak h_1', which originates from the $^2\Pi_{1/2u}$ anion ground state but overlaps with a SO peak.

Our assignments of the vibrational origin 0_0^0 (peak A), symmetric stretch 2_0^1 (peak I), and doubly excited bending modes 5_0^2 (peaks d_1 and d_2), 6_0^2 (peaks m_1 and m_2), and 7_0^2 (peaks c_1 and c_2) agree with those of Kitsopoulos *et al.*[45] The ZEKE spectrum also showed a combination band assigned as $5_0^2 7_0^2$. In the analysis presented here, this transition (peak H) is reassigned as $6_0^1 7_0^1$, and a weak feature (peak h_1') overlapping the $6_0^1 7_0^1$ SO peak (peak h_2') is assigned to $5_0^2 7_0^2$, in better agreement with the location and strength of the transitions predicted by the FC simulation. We also observe the $2_0^1 7_0^2$ (peaks l_1 and l_2) and $6_0^2 7_0^2$ (peaks p_1 and p_2) combination bands, as well as the more tentatively assigned features: 5_0^4 (peak J), $6_0^1 7_0^3$ (peak K), $2_0^1 5_0^2$ (peak N), and $2_0^1 7_0^4$ (peak O). The assignment of peaks N and O is especially uncertain, as both lie close to the expected energies of the $2_0^1 5_0^2$ and $2_0^1 7_0^4$ transitions. The simulation predicts $2_0^1 5_0^2$ to be the more intense of the two transitions, but the predicted energy of this feature is closer to peak N, the less intense peak.

There are two weak features (peaks B and F) in the low-resolution SEVI spectrum that do not appear in the high-resolution spectra. Both peaks are assigned to transitions to a neutral state with a single quantum of excitation in a π_u bending mode: peak B to 7_0^1 and peak F to 6_0^1. These peaks can only appear through a vibronic coupling process, as discussed in more detail below.

The high-resolution traces presented in Fig. 1 also show closely spaced splittings of the vibrational states of C_5 with multiple quanta in doubly degenerate bending modes. These splittings are most reasonably assigned to states with the same vibrational quantum number but different vibrational angular momenta. Our spectra represent the first resolution of vibrational angular momentum structure in C_5, though such structure has been seen in similar systems such as C_3[66,67] and carbon suboxide (C_3O_2).[68–70] An approximate energy formula for the excitation of doubly degenerate vibrations in a molecule is given by[71]

$$G(n_1, n_2, \ldots) = \sum_i \nu_i(n_i + d_i/2) + \sum_i \sum_{k \geq i} x_{ik}(n_i + d_i/2) \times (n_k + d_k/2) + \sum_i \sum_{k \geq i} g_{ik} l_i l_k + \ldots, \quad (1)$$

where ν_i is the harmonic frequency of the ith mode, n_i is the vibrational quantum number of the ith mode, d_i is the degeneracy of the ith mode, x_{ik} and g_{ik} are small constants giving corrections to account for anharmonicity, and $l_i = \{-n_i, -n_i + 2, \ldots, n_i - 2, n_i\}$ is the vibrational angular momentum of the ith mode.

The most straightforward case of vibrational angular momentum structure in the C_5 spectra occurs for transitions to a doubly degenerate bending mode ν_i with $n_i = 2$, where $i = \{5, 6, 7\}$. In this case $l_i = \{0, \pm 2\}$; the $l_i = 0$ state has σ_g^+ vibrational symmetry and the $l_i = \pm 2$ states have δ_g symmetry. In a perfectly harmonic potential, all three levels with $n_i = 2$ would be degenerate in energy, but to the order of accuracy given in Eq. (1), anharmonicity causes a splitting of $4g_{ii}$ between the $l_i = 0$ and $l_i = \pm 2$ states. Splittings observed for the 5_0^2, 6_0^2, and 7_0^2 transitions in the SEVI spectra of C_5^- are reported in Table II. The SO-excited peak of 6_0^2 is intense enough to reveal a splitting as well (peaks m_1' and m_2' in inset of Fig. 1). The splitting of the doubly excited ν_7 mode is also seen for $2_0^1 7_0^2$ (peak L); ν_2 is a σ_g^+ stretching mode and therefore does not appear to alter the vibrational angular momentum structure of the 7_0^2 transition when observed in combination. In all cases mentioned above, the peak at lower eBE is more intense, and is assigned to the $l_i = 0$ state since this transition is nominally FC allowed, whereas transitions to the $l_i = \pm 2$ levels are not (see below).

The $6_0^2 7_0^2$ transition (peaks p_1 and p_2) has a complicated multiplet structure not fully resolved in the SEVI spectra. This is befitting of a state involving two quanta of excitation in each of two doubly degenerate vibrational modes, which within the approximation of Eq. (1) should result in a quintuplet. We expect 5_0^4 (peak J), 7_0^4 (peak E), and $6_0^1 7_0^3$ (peak K) to show similar multiplet structure, but they are too weak to resolve any splittings. It is also possible that peaks N and O, tentatively assigned to $2_0^1 5_0^2$ and $2_0^1 7_0^4$, are in fact the angular momentum multiplet of a single vibrational transition.

Equation (1) predicts the $6_0^1 7_0^1$ transition (peak H) to appear as a doublet split by $2g_{67}$. We resolve peak H as a singlet with a 7 cm^{-1} FWHM. High-resolution IR spectroscopy studies of the closely related carbon suboxide (C_3O_2) molecule have observed vibrational angular momentum splittings of less than 3 cm^{-1} for the analogous $\nu_6 + \nu_7$ mode.[68,70] Splittings of this magnitude cannot be resolved with our SEVI spectrometer, so we expect $6_0^1 7_0^1$ to appear as a singlet.

There are several features in the SEVI spectra that are not reproduced in the FC simulations. In addition, the simulated intensities for many of the transitions that are reproduced are systematically lower than the experimental intensities. Some of these discrepancies can be addressed by varying the geometries obtained from the electronic structure calculations. For example, increasing the calculated outer C–C bond length of the anion by 0.01 Å boosts the simulated intensity of the 2_0^1 transition (peak I) by nearly 50%. However, so long as the anion and neutral are linear, odd Δn transitions in the bending modes are FC forbidden.[72] Moreover, one cannot significantly affect the intensities of FC allowed (even Δn) transitions involving the bending vibrations without drastic alteration of the anion and neutral bend frequencies listed in Table II. It is more likely that these systematic intensity discrepancies are caused by vibronic coupling effects in the neutral and anion.

We first consider peaks B and F, which are assigned to the 7_0^1 and 6_0^1 transitions, respectively. These transitions are FC forbidden. However, the neutral levels have overall Π_u vibronic symmetry. Transitions to these levels can occur if they are mixed by Herzberg-Teller (HT) coupling with totally symmetric vibrational levels of a low-lying $^1\Pi_u$ excited electronic state of C_5. Such a state has been predicted by theory to lie ~2.6 eV above the $^1\Sigma_g^+$ electronic ground state[29] and has been observed for C_5 in a neon matrix and in the gas phase with a term energy of ~2.43 eV.[21–23]

A photodetachment transition from a $^2\Pi_u$ anion electronic state that is allowed by HT coupling with a $^1\Pi_u$ state would yield an outgoing photoelectron wavefunction with π_u symmetry.[64,65] Indeed, peaks B and F have parallel PADs corresponding to p-wave detachment. Additionally, the near-threshold cross section for photodetachment (σ) is governed by the Wigner threshold law,[73] $\sigma \propto (eKE)^{l+1/2}$, where l is the angular momentum of the outgoing photoelectron. As a result, the photodetachment cross section falls off more sharply close to threshold for p-wave ($l = 1$) electrons than for s-wave ($l = 0$) electrons. Peaks B and F are therefore expected to vanish close to threshold, as they do in the high-resolution SEVI spectra. More detailed discussions of vibronic coupling among neutral electronic states in photoelectron spectra and SEVI experiments are presented in Refs. 57, 74, and 75.

The appearance of the FC forbidden $l_i = \pm 2$ components of the i_0^2 transitions and the unexpected strength of their $l_i = 0$ components is attributed to a different vibronic coupling scheme: Renner-Teller coupling between the vibrational levels of the anion within its $^2\Pi_u$ electronic ground state. Renner-Teller coupling between vibrational levels in Π electronic states of linear molecules is well-understood.[40,76,77] It is usually invoked to explain complex shifting and splitting of vibrational and rotational structure within a Π state. In the case of the SEVI spectra of C_5^-, however, RT coupling appears in a somewhat novel way, as a means of providing intensity to weak or forbidden vibronic transitions.

RT coupling in the C_5^- anion has been discussed in detail by Perić *et al.*[40] If the anion electronic orbital angular momentum (Λ) and the vibrational angular momenta of the bending modes are allowed to mix, Λ and l_i are no longer good quantum numbers. Instead one must consider the vibronic angular momentum $K = |l_5 + l_6 + l_7 + \Lambda|$. The anion ground vibrational state can couple to both the $l_i = 0$ and $l_i = \pm 2$ states for anion bending modes with $n_i = 2$, as all have components with Π_u overall vibronic symmetry and $K = 1$. The matrix elements $\langle n_i = 0, l_i = 0 | \hat{H} | n_i = 2, l_i = 0, \pm 2 \rangle$ of the anion Hamiltonian can therefore be non-zero for modes ν_5, ν_6, and ν_7. This coupling scheme is laid out in Fig. 2 for the case of a π_u bending mode. Such a scheme enables transitions from the anion vibrational ground state to the doubly excited bending modes of the neutral with $l_i = \pm 2$. Transitions to neutral bending modes with $n_i = 2$, $l_i = 0$ would also appear more intense than predicted by FC simulation as a result of this coupling, as seen in our spectra.

The situation is very similar for a single quantum of excitation in each of two distinct π_u modes such as the $6_0^1 7_0^1$ transition (peak H). This combination results in three states with vibrational symmetry σ_g^+, σ_g^-, and δ_g, and since l_6, $l_7 = \pm 1$, we have $l_{tot} = l_6 + l_7 = \{0, \pm 2\}$.[71] All three states are of the correct symmetry to couple vibronically with the anion ground vibrational state, and may therefore appear in the neutral spectra through RT coupling, as in the $n_i = 2$ case. As

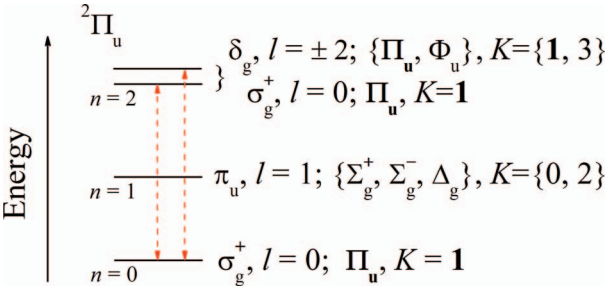

FIG. 2. Schematic of π_u bending mode levels in the C_5^- anion $^2\Pi_u$ electronic ground state, neglecting spin-orbit splittings and Renner-Teller splitting of the $n = 1$ level for the purpose of illustration. Labels indicate vibrational symmetry and angular momentum quantum number l for each level as well as the overall vibronic symmetry and K value. The ground vibrational state interacts with the $n = 2$, $l = \{0, \pm 2\}$ levels through RT coupling (marked in red), as those levels have components with the same overall Π_u vibronic symmetry and $K = 1$.

discussed previously, the energy splitting between the various l_{tot} states is too narrow to resolve with SEVI, and as a result, the $6_0^1 7_0^1$ peak appears as a singlet in the spectra. RT coupling is only possible in this case because the ν_6 and ν_7 bending modes are both of cis (i.e., π_u) symmetry.[40] The combination of a single excitation in both a trans mode and a cis mode (e.g., ν_5 and ν_6) would not result in states with the correct symmetry to RT couple with the anion ground vibrational state.

The FC forbidden δ_g peaks could conceivably be attributed to Herzberg-Teller coupling with totally symmetric vibrational levels of a $^1\Delta_g$ excited state of C_5. However, the lowest lying $^1\Delta_g$ state of C_5 has been calculated to lie ~4.5 eV above the C_5 ground state.[29] Such a state would seem too far removed to support what would need to be a strong vibronic coupling with the ground state, since the forbidden $n_i = 2$, $l_i = \pm 2$ bending mode peaks appear nearly as intense as the $n_i = 2$, $l_i = 0$ peaks. Additionally, unlike the proposed Renner-Teller scheme, HT coupling would not explain why all multiply excited bending mode features appear more strongly than predicted by the FC simulation.

VI. CONCLUSIONS

High-resolution SEVI spectra of cryogenically cooled C_5^- clusters are reported. We identify the ν_2 symmetric stretching mode, doubly excited ν_5, ν_6, and ν_7 bending modes, and various combination bands of the neutral C_5 cluster. Coupled cluster electronic structure theory calculations and Franck-Condon simulations are in sufficient agreement with the experimental spectrum to enable assignment of most of the observed features. Additionally, we resolve vibrational angular momentum structure of various multiply excited bending modes which can only appear through Renner-Teller coupling between vibrational levels of the anion electronic ground state, and two FC forbidden π_u vibrational modes which must appear through Herzberg-Teller coupling between electronic levels of the neutral cluster.

The ability to resolve vibrational fine structure in size-selected clusters shows that slow photoelectron velocity-map imaging has considerable potential for cluster spectroscopy, as demonstrated here and, very recently, by Wang and coworkers for Au_4^-.[78] This capability is dramatically enhanced by the cryo-cooling method described in this work.

ACKNOWLEDGMENTS

This research is funded by the Air Force Office of Scientific Research under Grant No. FA9550-12-1-0160 and the Defense University Research Instrumentation Program under Grant No. FA9550-11-1-0300. M.L.W. thanks the National Science Foundation for a graduate research fellowship.

[1] W. Weltner, Jr. and R. J. Van Zee, Chem. Rev. **89**, 1713 (1989).
[2] R. P. A. Bettens and E. Herbst, Astrophys. J. **478**, 585 (1997).
[3] A. Van Orden and R. J. Saykally, Chem. Rev. **98**, 2313 (1998).
[4] E. B. Jochnowitz and J. P. Maier, Annu. Rev. Phys. Chem. **59**, 519 (2008).
[5] A. G. G. M. Tielens, Rev. Mod. Phys. **85**, 1021 (2013).
[6] C. Hock, J. B. Kim, M. L. Weichman, T. I. Yacovitch, and D. M. Neumark, J. Chem. Phys. **137**, 244201 (2012).
[7] J. B. Kim, C. Hock, T. I. Yacovitch, and D. M. Neumark, J. Phys. Chem. A **117**, 8126 (2013).
[8] K. S. Pitzer and E. Clementi, J. Am. Chem. Soc. **81**, 4477 (1959).
[9] K. Raghavachari and J. S. Binkley, J. Chem. Phys. **87**, 2191 (1987).
[10] J. M. L. Martin and P. R. Taylor, J. Phys. Chem. **100**, 6047 (1996).
[11] R. E. Smalley, Acc. Chem. Res. **25**, 98 (1992).
[12] G. von Helden, M. T. Hsu, N. Gotts, and M. T. Bowers, J. Phys. Chem. **97**, 8182 (1993).
[13] G. Pacchioni and J. Koutecký, J. Chem. Phys. **88**, 1066 (1988).
[14] J. Kurtz and L. Adamowicz, Astrophys. J. **370**, 784 (1991).
[15] M. Vala, T. M. Chandrasekhar, J. Szczepanski, R. Van Zee, and W. Weltner, Jr., J. Chem. Phys. **90**, 595 (1989).
[16] P. F. Bernath, K. H. Hinkle, and J. J. Keady, Science **244**, 562 (1989).
[17] J. R. Heath, A. L. Cooksy, M. H. Gruebele, C. A. Schmuttenmaer, and R. J. Saykally, Science **244**, 564 (1989).
[18] N. Moazzen-Ahmadi, A. R. W. McKellar, and T. Amano, J. Chem. Phys. **91**, 2140 (1989).
[19] R. H. Kranze and W. R. M. Graham, J. Chem. Phys. **96**, 2517 (1992).
[20] J. Szczepanski, S. Ekern, C. Chapo, and M. Vala, Chem. Phys. **211**, 359 (1996).
[21] D. Forney, P. Freivogel, M. Grutter, and J. P. Maier, J. Chem. Phys. **104**, 4954 (1996).
[22] T. Motylewski, O. Vaizert, T. F. Giesen, H. Linnartz, and J. P. Maier, J. Chem. Phys. **111**, 6161 (1999).
[23] A. E. Boguslavskiy and J. P. Maier, J. Chem. Phys. **125**, 094308 (2006).
[24] P. Botschwina and P. Sebald, Chem. Phys. Lett. **160**, 485 (1989).
[25] P. Botschwina, J. Chem. Phys. **101**, 853 (1994).
[26] M. Kolbuszewski, J. Chem. Phys. **102**, 3679 (1995).
[27] P. Botschwina, Theor. Chem. Acc. **104**, 160 (2000).
[28] M. Hanrath and S. D. Peyerimhoff, Chem. Phys. Lett. **337**, 368 (2001).
[29] H. Massó, V. Veryazov, P.-Å. Malmqvist, B. O. Roos, and M. L. Senent, J. Chem. Phys. **127**, 154318 (2007).
[30] L. Adamowicz, Chem. Phys. Lett. **180**, 466 (1991).
[31] J. D. Watts and R. J. Bartlett, J. Chem. Phys. **97**, 3445 (1992).
[32] M. Ohara, H. Shiromaru, Y. Achiba, K. Aoki, K. Hashimoto, and S. Ikuta, J. Chem. Phys. **103**, 10393 (1995).
[33] M. Tulej, D. A. Kirkwood, G. Maccaferri, O. Dopfer, and J. P. Maier, Chem. Phys. **228**, 293 (1998).
[34] N. M. Lakin, F. Güthe, M. Tulej, M. Pachkov, and J. P. Maier, Faraday Discuss. **115**, 383 (2000).
[35] J. Szczepanski, S. Ekern, and M. Vala, J. Phys. Chem. A **101**, 1841 (1997).
[36] P. Freivogel, M. Grutter, D. Forney, and J. P. Maier, Chem. Phys. **216**, 401 (1997).
[37] D. Forney, M. Grutter, P. Freivogel, and J. P. Maier, J. Phys. Chem. A **101**, 5292 (1997).
[38] M. G. Giuffreda, M. S. Deleuze, and J.-P. François, J. Phys. Chem. A **106**, 8569 (2002).
[39] Z. Cao, S. D. Peyerimhoff, F. Grein, and Q. Zhang, J. Chem. Phys. **115**, 2062 (2001).
[40] M. Perić, M. Petković, and S. Jerosimić, Chem. Phys. **343**, 141 (2008).
[41] D. G. Leopold, J. Ho, and W. C. Lineberger, J. Chem. Phys. **86**, 1715 (1987).

[42]A. W. Castleman, Jr., and K. H. Bowen, Jr., J. Phys. Chem. **100**, 12911 (1996).
[43]S. Yang, K. J. Taylor, M. J. Craycraft, J. Conceicao, C. L. Pettiette, O. Cheshnovsky, and R. E. Smalley, Chem. Phys. Lett. **144**, 431 (1988).
[44]D. W. Arnold, S. E. Bradforth, T. N. Kitsopoulos, and D. M. Neumark, J. Chem. Phys. **95**, 8753 (1991).
[45]T. N. Kitsopoulos, C. J. Chick, Y. Zhao, and D. M. Neumark, J. Chem. Phys. **95**, 5479 (1991).
[46]A. Osterwalder, M. J. Nee, J. Zhou, and D. M. Neumark, J. Chem. Phys. **121**, 6317 (2004).
[47]D. M. Neumark, J. Phys. Chem. A **112**, 13287 (2008).
[48]U. Even, J. Jortner, D. Noy, N. Lavie, and C. Cossart-Magos, J. Chem. Phys. **112**, 8068 (2000).
[49]D. Gerlich, *Advances in Chemical Physics* (Wiley, 1992), pp. 1–176.
[50]W. C. Wiley and I. H. McLaren, Rev. Sci. Instrum. **26**, 1150 (1955).
[51]A. T. J. B. Eppink and D. H. Parker, Rev. Sci. Instrum. **68**, 3477 (1997).
[52]D. W. Chandler and P. L. Houston, J. Chem. Phys. **87**, 1445 (1987).
[53]NuACQ, M. B. Doyle, C. Abeyasera, and A. G. Suits, see http://chem.wayne.edu/suitsgroup/NuACQ.html.
[54]B.-Y. Chang, R. C. Hoetzlein, J. A. Mueller, J. D. Geiser, and P. L. Houston, Rev. Sci. Instrum. **69**, 1665 (1998).
[55]E. W. Hansen and P. L. Law, J. Opt. Soc. Am. A **2**, 510 (1985).
[56]C. Blondel, C. Delsart, and F. Goldfarb, J. Phys. B **34**, 2757 (2001).
[57]J. B. Kim, M. L. Weichman, T. I. Yacovitch, and D. M. Neumark, J. Chem. Phys. **139**, 104301 (2013).
[58]P. J. Knowles, C. Hampel, and H. J. Werner, J. Chem. Phys. **99**, 5219 (1993).
[59]J. D. Watts, J. Gauss, and R. J. Bartlett, J. Chem. Phys. **98**, 8718 (1993).
[60]R. A. Kendall, T. H. Dunning, and R. J. Harrison, J. Chem. Phys. **96**, 6796 (1992).
[61]H.-J. Werner, P. J. Knowles, G. Knizia, F. R. Manby, M. Schütz *et al.*, MOLPRO, version 2010.1, a package of *ab initio* programs, 2010, see http://www.molpro.net.
[62]V. A. Mozhayskiy and A. I. Krylov, ezSpectrum 3.0, see http://iopenshell.usc.edu/downloads.
[63]F. Duschinsky, Acta Physicochim. URSS **7**, 551 (1937).
[64]E. Surber, R. Mabbs, and A. Sanov, J. Phys. Chem. A **107**, 8215 (2003).
[65]R. Mabbs, E. R. Grumbling, K. Pichugin, and A. Sanov, Chem. Soc. Rev. **38**, 2169 (2009).
[66]E. A. Rohlfing and J. E. M. Goldsmith, J. Opt. Soc. Am. B **7**, 1915 (1990).
[67]F. J. Northrup and T. J. Sears, J. Opt. Soc. Am. B **7**, 1924 (1990).
[68]P. Jensen and J. W. C. Johns, J. Mol. Spectrosc. **118**, 248 (1986).
[69]J. Vander Auwera, J. W. C. Johns, and O. L. Polyansky, J. Chem. Phys. **95**, 2299 (1991).
[70]J. Vander Auwera, J. K. Holland, P. Jensen, and J. W. C. Johns, J. Mol. Spectrosc. **163**, 529 (1994).
[71]G. Herzberg, *Molecular spectra and molecular structure. Vol. 2: Infrared and Raman spectra of polyatomic molecules* (D. Van Nostrand Co., Inc., New York, 1945).
[72]G. Herzberg, *Molecular spectra and molecular structure. Vol. 3: Electronic spectra and electronic structure of polyatomic molecules* (Van Nostrand Reinhold Co., New York, 1966).
[73]E. P. Wigner, Phys. Rev. **73**, 1002 (1948).
[74]K. M. Ervin and W. C. Lineberger, J. Phys. Chem. **95**, 1167 (1991).
[75]K. Klein, E. Garand, T. Ichino, D. M. Neumark, J. Gauss, and J. F. Stanton, Theor. Chem. Acc. **129**, 527 (2011).
[76]C. Jungen and A. J. Merer, Mol. Phys. **40**, 1 (1980).
[77]S. G. He and D. J. Clouthier, J. Chem. Phys. **123**, 014316 (2005).
[78]Z. Yang, I. Leon, and L.-S. Wang, J. Chem. Phys. **139**, 021106 (2013).